Signal transduction protein PII from Synechococcus elongatus PCC 7942 senses low adenylate energy charge in vitro.

Oleksandra Fokina, Christina Herrmann, Karl Forchhammer

Signal transduction protein P_{II} from *Synechococcus elongatus* PCC 7942 senses low adenylate energy charge *in vitro*.

Short title: Adenylate energy charge sensing by cyanobacterial P_{II} protein

Oleksandra Fokina, Christina Herrmann and Karl Forchhammer[1]

Interfakultäres Institut für Mikrobiologie und Infektionsmedizin der Eberhard-Karls-Universität Tübingen, Auf der Morgenstelle 28, 72076 Tübingen, Germany

Synopsis

P_{II} proteins belong to a family of highly conserved signal transduction proteins widely spread in bacteria, archaea and plants. They respond to the central metabolites ATP, ADP and 2-oxoglutarate (2-OG) and control enzymes, transcription factors and transport proteins involved in nitrogen metabolism. Here we studied the effect of ADP on *in vitro* P_{II} signalling properties from the cyanobacterium *Synechococcus elongatus*, a model for oxygenic phototrophic organisms. Different ADP/ATP ratios strongly affected the properties of P_{II} signalling. Increasing ADP antagonized the binding of 2-oxoglutarate and directly affected the interactions of P_{II} with its target proteins. The resulting P_{II} signalling properties indicate that in mixtures of ADP and ATP, P_{II} trimers are occupied with mixtures of adenylate nucleotides. Binding and kinetic activation of *N*-acetyl-L-glutamate kinase (NAGK) (the controlling enzyme of arginine biosynthesis) by P_{II} was weakened by ADP, but relief from arginine inhibition remained unaffected. On the other hand, ADP enhanced the binding of P_{II} to PipX, a co-activator of transcription factor NtcA and furthermore, antagonised the inhibitory effect of 2-OG on P_{II}-PipX interaction. These results indicate that *S. elongatus* P_{II} directly senses the adenylate energy charge, resulting in target-dependent differential modification of the P_{II} signalling properties.

Key words: metabolic signalling, nitrogen regulation, 2-oxoglutarate, P_{II} protein, energy charge, cyanobacteria

Abbreviations used: EC, energy charge; 2-OG, 2-oxoglutarate; NAGK, *N*-acetyl-L-glutamate kinase; SPR, surface plasmon resonance; ITC, isothermal titration calorimetry; FC, flow cell; RU, resonance units; NAG, *N*-acetyl-L-glutamate

[1]To whom correspondence should be addressed (email karl.forchhammer@uni-tuebingen.de)

Introduction

ATP in the cell provides energy for metabolic reactions, serves as a substrate for nucleotide synthesis and regulates cell metabolism as a signal molecule. The adenylate energy charge (EC), [(adenosine triphosphate) + (adenosine diphosphate)]/[(adenosine triphosphate) + (adenosine diphosphate) + (adenosine monophosphate)] is a measure of the energy available for metabolism [1]. Since in bacteria the concentration of AMP is constantly low, the adenylate energy charge depends mainly on the ATP/ADP ratio [2]. However, sensors of the adenylate energy charge have been poorly characterized. Recently the P_{II} signal transduction proteins have been suggested to be involved in EC measurement. They respond to ATP, ADP and 2-oxoglutarate (2-OG) by binding these effectors in an interdependent manner [3-7], thereby transmitting metabolic information into structural states of the P_{II} sensor protein [8, 9]. P_{II} when fully occupied by either ATP or ADP corresponds to non-physiological extremes of EC. To understand how P_{II} responds to physiologically relevant changes in EC, experiments must be conducted with different ATP/ADP ratios that span physiological conditions.

P_{II} signal transduction proteins are widely distributed in bacteria, archaea and the chloroplasts of eukaryotes, where they regulate metabolic and regulatory enzymes, transcription factors and/or transport proteins [4, 10-12]. In addition to responding to the metabolites ATP, ADP and 2-oxoglutarate (2-OG), P_{II} proteins can furthermore be subjected to signal-dependent reversible covalent modification, which occurs on the large surface exposed T-loop [10, 13]. P_{II} proteins are compact homotrimers with each subunit exposing three surface-exposed loops, termed T-loop, B-loop and C-loop [4]. The large T-loop is highly flexible and adopts different conformations, taking part in binding of effector molecules and being the dominating structure in protein-protein interactions. The B- and C-loops from opposite subunits are facing each other in the intersubunit cleft and take part in adenylate nucleotide binding [14-16]. The P_{II} trimer contains three adenylate nucleotide-binding sites, one in each intersubunit cleft, with ATP and ADP competing for the same site. In the presence of Mg^{2+}-ATP, up to three 2-OG molecules can bind to the protein at the base of the T-loop in direct vicinity of the beta and gamma-phosphate of ATP, which ligate 2-OG through a bridging Mg^{2+} ion [8-10]. Through this type of interaction, binding of ATP and 2-OG at one effector molecule binding site is synergistic towards each other. However, the three effector molecule binding sites exhibit negative cooperativity towards each other [3, 6, 17, 18]. The anticooperativity is mediated via intersubunit signalling [19]. First structural insight in this process was obtained recently for sequential 2-OG binding [8]. Occupation of the first, high affinity site, creates structural differences in the two neighboring sites, with one site displaying a clear distortion in the conformation of the bound ATP molecule. The anticooperativity in the binding of the effector results in a subsensitive response of this stimulatory effect, which is ideal for accurate detection of a wide range of metabolite concentrations.

Adenyl nucleotide binding seems to be highly similar in all P_{II} proteins from the three domains of life. In bacterial P_{II} proteins, ADP generally does not support 2-OG binding [3, 7], whereas in a plant P_{II} protein (*Arabidopsis thaliana*) 2-OG binding was supported both by ATP and ADP [20]. Effects of different ADP/ATP ratios have so for only been studied *in vitro* with *E. coli* P_{II} protein [3, 18]. Increasing ADP levels act antagonistically to 2-OG in the UTase/UR-P_{II}-NRII-NRI signal transduction cascade *in vitro*. Furthermore, ADP acts through P_{II} as an activator of ATase catalyzed glutamine synthetase adenylylation in the ATase-GS monocycle. On the other hand, the uridylylation of P_{II} by UTase is negatively influenced by ADP [3]. ADP increases the stability of the complex of the P_{II}-family protein GlnK with the ammonium channel AmtB and antagonizes the effect of 2-OG, pointing at the P_{II} sensing of the adenylate energy charge [7]. In the photosynthetic bacterium *Rhodospirillum rubrum,* three P_{II} homologues are involved in the regulation of the transcription activator NifA and the DRAT/DRAG system for the posttranslational regulation of nitrogenase activity [21-23]. The DRAT/DRAG system responds to the energy state, pointing towards a connection of P_{II} with the energy status in the cell [22]. However, there is only slight

impact of low ATP levels alone on the P_{II} regulation of both processes, supposedly, the ratio of ADP/ATP is significant this response [5].

In cyanobacteria P_{II} is involved in nitrate utilization [24, 25], regulation of gene expression by sequestering the co-activator PipX of the general transcription factor NtcA [26-28], and in arginine biosynthesis by regulating the controlling enzyme, *N*-acetyl-L-glutamate kinase (NAGK) [29, 30]. Binding of P_{II} from the cyanobacterium *Synechococcus elongatus* enhances the activity of NAGK and relieves it from feedback inhibition by arginine [31]. In higher plants, P_{II} also regulates NAGK [32] and, moreover, *A. thaliana* P_{II} binds and inhibits a key enzyme of fatty acid metabolism, acetyl-CoA carboxylase [33], representing another link between P_{II} and carbon metabolism. The structure of the P_{II}-NAGK complex, NAGK regulation by P_{II} and its response towards 2-OG are highly conserved between higher plants and cyanobacteria [34-36]. In the presence of Mg^{2+}-ATP, 2-OG strongly inhibits P_{II}-NAGK complex formation. Whereas in cyanobacteria, Mg^{2+}-ATP alone has only a slight effect on complex formation [6, 31], it favours the binding of P_{II} to NAGK in *A. thaliana* [20]. ADP accelerates the dissociation of the cyanobacterial proteins but has no major effect on the *A. thaliana* proteins [36].

The *S. elongatus* P_{II} protein is subjected to phosphorylation and dephosphorylation in response to the cellular 2-OG and ATP levels [37]. *In vitro*, high concentrations of 2-OG in presence of ATP cause phosphorylation of seryl-residue 49, an exposed residue at the apex of the T-loop [38]. The P_{II} kinase has not been identified yet. The phosphatase of P_{II}-P, PphA from *Synechocystis* PCC 6803, readily dephosphorylates P_{II}-P in the absence of effector molecules. This reaction is partially inhibited by ATP or ADP, but strongly by Mg^{2+}-ATP-2-OG [39]. Combining different mixtures of ADP/ATP and 2-OG revealed that the P_{II} dephosphorylation reaction responded highly sensitive towards the 2-OG levels, however changing the ATP/ADP ratio had only little effect [40], since both adenylate nucleotides inhibit the dephosphorylation reaction. In contrast, preliminary data indicate that ATP and ADP antagonistically influence the binding of P_{II} with its targets NAGK or PipX. This could indicate that the interaction of P_{II} with its downstream signalling targets is indeed responsive to the ATP/ADP level, as was reported for the interaction of the P_{II} protein from *E. coli* with its targets NtrB and ATase [3].

In this study we investigate the ability of *S. elongatus* P_{II} to act as an EC sensor *in vitro*, and found that indeed it has such ability. Interestingly, the two targets, NAGK and PipX, respond differently to changing ADP/ATP ratios, with PipX being more sensitive towards low ADP levels. Furthermore, we observed that the effects of EC were mediated both indirectly, by changing the 2-OG binding properties of P_{II}, and directly, by the alteration of P_{II} output activities upon the binding of mixtures of nucleotides to P_{II}.

Experimental

Construction of heterotrimeric P_{II} protein

Heterotrimeric P_{II}-proteins, consisting of the Strep-tagged and non-tagged subunits were constructed as follows: two *glnB* genes from *Synechococcus elongatus*, one carrying Strep-tag fusion, another without Strep-tag, were cloned into pETDuet-1 vector (Merck KGaA, Darmstadt, Germany). First, native *glnB* was amplified using primers containing *AatII* and *AvrII* restriction sites: P_{II}nfwd2 (5′-ATGCGACGTCGATAACGAGGGCAAAA-3′) and P_{II}nrev2 (5′-ATGCCCTAGGGTAAACGGCAGACAAA-3′). The PCR product was restricted with *AatII* and *AvrII* and cloned into multiple cloning site 2 (MCS2) of pETDuet-1 vector. The resulting plasmid was restricted with *NcoI* and *HindIII* for the insertion of Strep-tag-fused *glnB* into multiple cloning site 1 (MCS1). The amplification of the second gene was done using following primers: P_{II}sfor (5′-ATGCCCATGGTTACCACTCCCTATCAGT-3′) and P_{II}srev (5′-ATGCAAGCTTCGCAGTAGCGGTAAAC-3′). The clones were checked by sequencing with the primers pET-Upstream (5′-ATGCGTCCGGCGTAGA-3′) for MCS1 and T7-Terminator (5′-GCTAGTTATTGCTCAGCGG-3′) for MCS2.

Overexpression and purification of recombinant P_{II}, NAGK, PipX and AGPR

The *glnB* gene *from Synechococcus elongatus*, cloned into the Strep-tag fusion vector pASK-IBA3 (IBA, Göttingen, Germany), was overexpressed in *E. coli* RB9060 [41] and purified using affinity chromatography as described previously [30]. The His_6-tagged recombinant NAGK from *S. elongatus,* His_6-tagged PipX and N-acetylglutamate-5-phosphate-reductase (AGPR) from *E. coli* were overexpressed in *E. coli* strain BL21(DE3) [42] and purified as reported previously [26, 30, 43]. Heterotrimeric P_{II} was overexpressed in *E. coli* strain BL21(DE3) and purified as described above with following modification: protein elution was made with a gradient of 30 µM, 200 µM and 1 mM desthiobiotin, and analysed by SDS-PAGE. P_{II} trimers with one/two Strep-tags were localized in 200 µM desthiobiotin fractions.

Surface Plasmon Resonance Detection (SPR)

SPR experiments were performed using a BIAcore X biosensor system (Biacore AB, Uppsala, Sweden) at 25°C in HBS-Mg buffer containing 10 mM HEPES, 150 mM NaCl, 1 mM $MgCl_2$ and 0.005% Nonidet P-40, pH 7.5 as described previously [31]. The purified His_6-NAGK was immobilized on the Ni^+-loaded NTA sensor chip to flow cell 2 (FC2) in a volume of 50 µl at a concentration of 30 nM (hexamer) to receive a binding signal of approximately 3000 resonance units (RU), which corresponds to a surface concentration change of 3 ng/mm^2. To determine the influence of different ATP/ADP ratios on the association and dissociation of the P_{II}-NAGK complex, a solution of 100 nM P_{II} was injected over the sensor-chip immobilized His_6-NAGK surface in the presence of 2 mM ATP with 0, 1, 2, 3, or 4 mM ADP as well as in the presence of 2 mM ADP alone. P_{II} was afterwards eluted by an injection of the same proportion of the metabolites. Furthermore, 100 nM P_{II} was bound over the immobilized NAGK with or without 1 mM ADP and eluted by an injection of 1 mM ADP. To load fresh proteins on the NTA sensor chip, bound proteins were first removed by injection of 25 µl of 0.4 M EDTA pH 7.5, subsequently, the chip could be loaded again with 5 mM Ni_2SO_4 solution and His_6-NAGK as described above.

P_{II}-PipX complex formation on the NTA chip was measured as described previously [26]. The His_6-PipX (500 nM) was preincubated with homotrimeric Strep-P_{II} (100 nM monomer) in the absence and in the presence of effectors and injected on the Ni^{2+}-loaded NTA chip. As a control, His_6-PipX was bound to the chip in the absence of P_{II}. The response difference between binding of His_6-PipX alone and in the presence of P_{II} at t = 197 s after start of the injection phase, was taken as a measure of protein binding.

To assay the binding of PipX to immobilized P_{II}, a CM5 sensor chip was treated with Amino Coupling Kit (Biacore AB, Uppsala, Sweden) to bind Strep-Tactin protein (50 µg/µl) in a volume 50 µl on the surface [28]. Thereafter, the purified heterotrimeric or homotrimeric-Strep-tagged P_{II} (40 ng/µl) was immobilized on the chip surface in flow cell 2 (FC2) in a volume of 20 µl. PipX (21 ng/µl) was injected in a volume of 20 µl in the presence of following effectors: 2 mM ADP, 2 mM ATP and 1 mM 2-OG. To remove P_{II} from the surface, the chip was washed with 5 mM desthiobiotin and regenerated by injecting HABA-buffer (IBA, Göttingen, Germany).

Isothermal Titration Calorimetry (ITC)

ITC experiments were performed on a VP-ITC microcalorimeter (MicroCal, LCC) in buffer containing 10 mM HEPES-NaOH, pH 7.4, 50 mM KCl, 50 mM NaCl and 1 mM $MgCl_2$ at 20°C.

Isotherms of 2-OG binding to P_{II} (33 µM trimer concentration) were determined in the presence of various ATP/ADP ratios: 1 mM/0.25 mM, 1 mM/0.5 mM, 1 mM/1 mM as well as only 1 mM ATP or 1 mM ADP. For one measurement 5 µl of 2 mM 2-OG was injected 35 times (4.2-293.7 µM) to the measuring cell containing P_{II} protein (cell volume 1.4285 ml) with stirring at 350 rpm. The binding isotherms were calculated from the recorded data and fitted to a one-site and a three-sites binding models using the MicroCal ORIGIN software (Northampton, USA) as indicated.

Direct coupled NAGK activity assay

The specific activity of NAGK from *S. elongatus* was assayed by coupling NAGK-dependent NAG phosphorylation to AGPR-catalyzed reduction of NAG-phosphate with NADPH as reductant and recording the change in absorbance at 340 nm [43]. The reaction buffer consisted of 50 mM potassium phosphate buffer (pH 7), 50 mM KCl, 20 mM $MgCl_2$, 0.2 mM NADPH and 0.5 mM DTT. Each reaction contained 10 µg AGPR, 50 mM NAG and 2.4 µg P_{II} with 6 µg NAGK or 1.2 µg P_{II} with 3 µg NAGK. The metabolites ATP, ADP, arginine and 2-OG varied depending on the experiment being performed. The reaction was started by the addition of NAGK. Phosphorylation of one molecule of NAG leads to oxidation of one molecule of NADPH, which is followed by the linear decrease of absorbance at 340 nm, recorded in a volume of 1 ml over a period of 10 min with a SPECORD 200 photometer (Analytik Jena). One unit of NAGK catalyzes the conversion of 1 mmol NAG per min. The reaction velocity was calculated with a molar absorption coefficient of NADH of ε_{340} = 6178 L mol^{-1} cm^{-1} from the slope of the change of absorbance per time.

P_{II}-PipX *in vitro* cross-linking

P_{II}-PipX interaction was analyzed using glutardialdehyde cross-linking. P_{II} (0.1 µg/µl) was preincubated with PipX (0.2 µg/µl) in the absence or in the presence of effectors ATP, ADP and 2-OG in 20 µl buffer containing 10 mM potassium phosphate buffer pH 7.4, 100 mM NaCl and 2 mM $MgCl_2$ at 4°C. After 5 min, 0.1% (w/w) glutardialdehyde was added and the samples were incubated for 5 min at 25°C. The cross-linking reaction was stopped by the addition of 100 mM Tris-HCl pH 7.4. The cross-link products were analyzed by 12.5% SDS-PAGE followed by immunoblot analysis with P_{II}-specific antibody as described previously [44].

Results

Different ATP/ADP ratios affect the activation of NAGK by P_{II} and its relief from arginine inhibition

The effect of different ADP/ATP ratios on the activation of NAGK by P_{II} and on the P_{II}-mediated relief from arginine inhibition could not be determined in the previously used assay, in which ATP consumption was coupled to NADH oxidation. However, by assaying the activity of NAGK in a reaction, where the phosphorylation of NAG is linked to the subsequent reduction of NAG-phosphate by AGPR with NADPH as a reductant [43], it is possible to determine the activity of NAGK under almost physiological conditions and at variable ATP/ADP levels. Increasing ATP concentrations from 0.5 mM to 4 mM enhanced the activity of NAGK both in the presence or absence of P_{II} (Fig. 1a and b), which was expected from the K_m of NAGK for ATP (without P_{II} K_m=0.6 mM, in the presence of P_{II} K_m=1.1 mM) [36]. Addition of ADP monotonically reduced the activity of P_{II}-complexed NAGK at any fixed ATP concentration. The higher the ADP concentration was, the more decreased the activity of NAGK. At a low constant ATP concentration, the relative decrease in NAGK activity by ADP addition was more pronounced than at high constant ATP concentration (6.4-fold decrease from 0 to 4 mM ADP at fixed 0.5 mM ATP compared to 2.6-fold decrease from 0 to 4 mM ADP at fixed 4 mM ATP). At the highest ADP/ATP ratio (4 mM ADP with 0.5. mM ATP), NAGK activity in presence of P_{II} was as low as NAGK activity in the absence of P_{II} (Fig. 1a and b). In the absence of P_{II}, NAGK responded only weakly to different ATP/ADP ratios (Fig. 1b), with a 1.8-fold reduction of activity comparing 0 and 4 mM ADP at any fixed ATP concentration. This indicates that the response of NAGK activity in presence of P_{II} towards different ADP/ATP ratios operates through the adenylate binding properties of P_{II}.

In the AGPR-coupled assay, NAGK was more sensitive to arginine inhibition than in the previously reported pyruvate kinase (PK)/ lactate dehydrogenase (LDH) coupled assay [31, 36], which keeps the ATP level constant at 10 mM. Using the AGPR-coupled assay, 10 µM arginine inhibited the free enzyme, but P_{II} relieved NAGK from arginine inhibition (Fig. 2a), as described previously for

the colorimetric assay and the PK/LDH coupled assay [31, 36]. The inhibitory effect of ADP on NAGK in the presence of P_{II} was tested at different arginine concentrations (20 µM, 40 µM and 60 µM), which are completely inhibitory for free NAGK but not or only moderately inhibitory to P_{II}-complexed NAGK. In these experiments ATP was fixed at 2 mM. Arginine inhibition was efficiently relieved by P_{II} in the presence of ATP alone; increasing concentrations of ADP increasingly diminished this effect, but didn't completely tune it down. If ADP would completely inhibit complex formation between P_{II} and NAGK, full inhibition of NAGK would be expected at high ADP concentrations in the presence of arginine. The lack of full inhibition implies that ADP did not fully prevent P_{II}-NAGK interaction in the presence of 2 mM ATP.

2-OG is a key effector molecule in P_{II} mediated signal transduction; micromolar amounts of 2-OG in the presence of ATP negatively affected P_{II}-NAGK complex formation [31]. Previous studies using the PK/LDH coupled assay could demonstrate the inhibitory effect of 2-OG on P_{II}-NAGK interaction by antagonizing the protective effect of P_{II} on NAGK activity in the presence of 50 µM arginine. In a similar experimental setting using the AGPR-coupled assay, NAGK activity decreased 10-fold when the 2-OG concentration was increased from 0 to 250 µM in the presence of P_{II}, 30 µM arginine and 2 mM ATP (Fig. 2b). The apparent half maximal inhibitory concentration (IC_{50}) of 2-OG was estimated to be 78 µM, a similar result as obtained in the previous study [6]. To reveal, how ADP affects the response towards 2-OG, the same experiment was performed in the presence of 2 mM ATP together with 2 mM ADP (Fig. 2b). The activity at zero 2-OG was 3-times lower than in the control in the absence of ADP, and it decreased 5-fold by titrating 2-OG up to 250 µM. The apparent IC_{50} for 2-OG in the presence of ADP was at about 145 µM, showing that 2-OG inhibited P_{II}-NAGK complex formation also in the presence of ADP, although moderately less efficiently.

Inhibitory effect of ADP on 2-OG binding of P_{II} in the presence of ATP

The 2-OG-binding site in P_{II} is created by a Mg^{2+} ion, which is coordinated by the gamma-phosphate of a bound ATP molecule and amino acid residues of one monomer of the P_{II} trimer itself. Binding of a single 2-OG molecule to P_{II} leads to a strong conformational change of the T-loop extending from the subunit, which ligates 2-OG, and moreover, to subtle changes in the other two binding sites as a result of negative cooperativity [8]. 2-OG binding in the presence of ATP was already measured by Isothermal Titration Calorimetry and the raw data could be fitted to a three sequential binding site model, that revealed the anticooperative occupation of the three binding sites [6]. Since ADP and ATP compete for the same binding site, an ADP molecule bound to one monomer of P_{II} might influence the affinity for 2-OG of the other two monomers because of the P_{II} intersubunit communication. Therefore, we next studied the effect of ADP on the binding of 2-OG to P_{II}. The raw data were tried to fit according to a three sequential binding model, but were also fitted using a one binding site model, because in a mixture of ATP and ADP, the number of available 2-OG-binding sites in P_{II} cannot be reliably predicted. Data fitting according to a model with three sequential binding sites could only be achieved for measurements done in excess of ATP over ADP (Table 1). At a molar ratio of 1:1 ADP/ATP, the binding isotherm was only consistent with the one-site model. Fitting to a one binding site model reveals a combined K_d of all binding sites and a mean stoichiometry of bound ligands. As shown in Fig. 3a, 2-OG exhibited high affinity towards P_{II} in the presence of 1 mM ATP. The combined K_d of 39 µM for all three binding sites was calculated from the binding isotherms of three independent experiments. On the other hand, in the presence of Mg^{2+}-ADP, titration with 2-OG didn't yield any calorimetric signals (Fig. 3b), obviously because ADP is not able to create the 2-OG-binding site. To reveal how ADP affects the binding of 2-OG to P_{II} in presence of ATP, 2-OG was titrated to various mixtures of ADP/ATP in presence of P_{II}. The addition of 0.25 mM ADP to 1 mM ATP (ADP/ATP ratio 1:4) had a negative effect on 2-OG binding (Fig 3c) with the apparent K_d increasing to 78 µM and the binding stoichiometry (N) decreasing from 1.73 to 1.35 (Table 1). Increasing concentrations of ADP led to further increase of the K_d for 2-OG binding and to a decrease in the binding stoichiometry (Fig 3d

and e, Table 1). In the presence of ATP alone, data fitting retrieved a mean stoichiometry of 1.73 2-OG molecules per P_{II} trimer. Since each P_{II} trimer has three binding sites for 2-OG, data fitting according to a one binding site model underestimates the actual number of binding sites, which could be due to the anticooperativity between the sites. The N value in the presence of 1 mM ATP and 1 mM ADP (1:1 ratio, N = 0.75) therefore indicates that one of the three binding sites can be efficiently occupied by 2-OG under theses conditions. Furthermore, ADP increases the K_d of the remaining 2-OG binding site to approximately 183 µM.

Different ATP/ADP ratios alter the association and dissociation of the P_{II}-NAGK complex

As shown previously, ADP negatively affects P_{II}-NAGK interaction by increasing the dissociation of the complex [6]. To reveal in more detail how ADP affects P_{II}-NAGK association, P_{II} was first loaded on the NAGK surface in the absence of effectors and was than eluted by injection of 1 mM ADP (Fig. 4a, left). Subsequently, the same amount of P_{II} was injected to the NAGK sensor surface in presence of 1 mM ADP, which resulted again in rapid complex formation. At the end of injection, after an initial drop of resonance units, dissociation ceased. A further injection of 1 mM ADP resulted again in rapid dissociation of bound P_{II} (Fig. 4a, right). Comparing the association curves shows that in presence of ADP, the curve reaches rapidly a plateau, which is approximately at one third of the maximal level obtained in absence of ADP. The steep initial increase of resonance units and rapid equilibration indicates that ADP enhances both the association and dissociation kinetics of P_{II}-NAGK complex formation. The fact that P_{II}-ADP didn't fully dissociate from NAGK after the end of the injection, but could again be rapidly dissociated after a further injection of ADP can be explained. At the end of the P_{II}-ADP injection, when the sensor ship is rinsed with ADP-free running buffer, ADP from P_{II} dissociates faster than P_{II}-ADP from NAGK, leaving ADP-free P_{II}, which can stay bound on NAGK.

The influence of various ADP/ATP ratios on P_{II}-NAGK interaction was investigated by injecting P_{II} on a sensor-chip with immobilized NAGK in the presence of different concentrations of ADP and ATP and subsequently injecting the same buffer in the absence of P_{II}, to determine the ATP/ADP-dependent dissociation of the complex (Fig. 4b). In the presence of ATP, rapid association of the P_{II}-NAGK was observed and injection of ATP to the complex didn't accelerate the dissociation. Addition of 1 mM ADP to 2 mM ATP had only a minor effect on complex formation (association was slightly faster and the maximal level slightly lower), but drastically accelerated complex dissociation (Fig. 4b). Higher concentrations of ADP (2 and 4 mM) at fixed 2 mM ATP lowered the steady state binding equilibrium during the first injection phase and increased the dissociation velocity to reach the velocity caused by ADP alone. Remarkably, in the excess of ADP over ATP, there was clearly more P_{II}-NAGK complex formation than with ADP alone, although complex dissociation was similarly fast in both cases.

Affinity of PipX to P_{II} in the presence of ADP

Three PipX monomers can bind to one P_{II} trimer in the absence of 2-OG [28]. However, at elevated 2-OG levels in the presence of ATP, P_{II}-PipX complex formation is impaired and free PipX can now bind to and activate the transcription factor NtcA [28]. These *in vitro* properties are correlated *in vivo* to nitrogen-limiting conditions. Here, we used SPR spectroscopy and glutardialdehyde cross-linking to determine the influence of ADP on 2-OG-modulated P_{II}-PipX complex formation.

In a first set of experiments, the His_6-PipX was preincubated with homotrimeric Strep-tagged P_{II} protein in the absence or in the presence of effectors and injected on the Ni^{2+}-loaded NTA chip. To ensure that all P_{II} trimers are fully occupied with PipX and enough free PipX is present, 5:1 PipX/P_{II} monomer ratio was used. In a control binding experiment His_6-PipX was loaded on the chip in the absence of P_{II}. PipX monomers alone showed relatively low binding to the chip due to the single short His_6-tag and therefore reached the equilibrium fast and dissociated after the end of the injection from the surface (Figure S1). Effectors had no influence on the interaction of His_6-PipX with Ni^{2+}-loaded NTA chip surface. Addition of P_{II} to PipX increased the binding signal in the sensorgram 2.5 times and decreased the dissociation rate, which can be explained by enhanced

binding of the P_{II}-PipX complexes, containing three His_6-tags that strongly bind to the surface, compared to monomeric PipX. P_{II} in the absence of PipX didn't bind to the chip surface. Thus, the increase of resonance units induced by the addition of P_{II} to PipX can be used to quantify P_{II}-PipX complex formation. Addition of 1 mM ADP to P_{II}-PipX had a strong positive effect on the binding signal, probably due to the stabilization of the P_{II}-PipX interaction, allowing more protein complexes to bind to the chip (Figure S1). The experiment was repeated in the presence of different ATD/ADP ratios and 2-OG. The increase of resonance units (ΔRU) from the start to the end of the injection indicates the amount of protein binding to the chip surface. The ΔRU values (at t = 197 s) for the binding of PipX without P_{II} was subtracted from the ΔRU values obtained in the presence of P_{II} and different effector molecules and the results are shown in the bar graph in Fig. 5a. In the absence of effectors the P_{II}-PipX complex binding reaches more than 800 RU. The amount of P_{II}-PipX complexes is enhanced by ADP and less efficiently by ATP; intermediate binding levels were obtained in a mixture of 1 mM ATP and ADP. Figure 5a shows that 2-OG in the presence of ATP is a strong inhibitor of P_{II}-PipX complex formation, the binding levels were almost the same as for free PipX. ADP acted antagonistically to 2-OG, even small amounts of ADP (0.05 mM) could significantly repress the 2-OG signal in the presence of 1 mM ATP *in vitro*. The amount of P_{II}-PipX complex in the presence of 1 mM ADP, ATP and 2-OG was even higher than in the absence of any effectors, showing that 1 mM ADP can almost completely erase the inhibitory effect of 2-OG.

This result was confirmed in a P_{II}-PipX binding assay, where proteins were preincubated under different conditions and cross-linked using glutardialdehyde. Subsequently, the products were visualized by SDS-PAGE and immunoblot analysis with P_{II}-specific antibody. As shown in Fig. 5b, in the absence of PipX, the cross-links of P_{II} trimers are prevalent and the dimeric form was only only slightly visible, the single P_{II} monomers were not present. Though in the presence of PipX alone no other bands were detected, with 1 mM ADP one additional band was observed, with higher molecular mass than the P_{II} trimer, consistent with a P_{II}-PipX cross-link product that could be formed, when ADP stabilized the complex. ATP had no such effect, but in the presence of both 1 mM ATP/ADP the characteristic band was also observed. In comparison to the SPR experiments, higher concentrations of ADP were needed to neutralize the negative effect of 2-OG.

The P_{II}-PipX interaction was also studied with C-terminal Strep-tagged P_{II} protein immobilized on a Strep-Tactin II-coated sensor chip surface, where PipX was injected as an analyte. Immobilized P_{II} protein was able to build a complex with PipX, but the interaction was insensitive to the effector molecules ATP and 2-OG (Fig. S2). We hypothesized, that by fixing the C-terminus of the P_{II} subunits on the chip surface, the conformational change of the C-terminus that occurs upon binding of ATP and 2-OG (a movement of the C-terminus towards the ATP-molecule) [8] is prevented and, therefore, the P_{II}-PipX complex was not affected by these effectors. To solve this question, a heterotrimeric Strep-tagged P_{II} protein was constructed by co-expressing Strep-tagged and untagged P_{II} subunits und purifying heterotrimers containing only one or two Strep-tagged subunits. If the above-mentioned assumption was true, the untagged subunits should be able to respond to the effectors. Heterotrimeric P_{II} was fixed on the Step-Tactin-coated chip and PipX could bind to this surface as efficient as to the homotrimeric Strep-tagged P_{II} protein (Fig. 5c). In contrast to the Strep-tagged P_{II} homotrimer, the interaction was indeed weakened by 1 mM 2-OG in the presence of 2 mM Mg^{2+}-ATP, although not completely, because of the remaining Strep-tagged P_{II} subunits. Injection of PipX in the presence of 2 mM ADP on the immobilized heterotrimeric P_{II} showed an enhanced velocity of complex association compared to binding in the absence of effector molecules. Furthermore, ADP was able to antagonize the negative effect of 2-OG on PipX-P_{II} binding: when ADP was added to a mixture of ATP and 2-OG, more PipX could bind to the P_{II} surface than in the absence of ADP.

Discussion

An important feature of cyanobacterial P_{II} signal transduction is the sensing of the balance of carbon and nitrogen status through binding of the central metabolite 2-OG. Results, presented here, indicate how P_{II} could also act as a sensor of adenylate energy charge in cyanobacteria. Binding of 2-OG to the ATP-ligated P_{II} protein is the fundament of P_{II}-mediated signal transduction. ADP was shown to occupy the ATP-site of P_{II} proteins [3, 14, 15]. Therefore, ADP binding prevents the coordination of the bridging Mg^{2+} ion by the γ-phosphate of ATP, which is essential for 2-OG binding [8]. In accord, no binding of 2-OG to ADP-occupied *S. elongatus* P_{II} protein occurs. When ATP and ADP are present simultaneously, as is the case in living cells, there will be competition for the three adenylate binding sites of the trimeric P_{II} protein. Moreover, it has to be considered, that the three binding sites are interacting in an anticooperative manner. In contrast to the *E.coli* system, where ADP binds better than ATP [3], the affinity of each of the three binding sites of the cyanobacterial P_{II} towards ADP (K_d of 10, 19 and 133 µM) is approximately 2-3 fold lower than towards ATP (K_d of 4, 12 and 47 µM) [6]. So, when P_{II} is exposed to a mixture of ATP and ADP, a mixed occupation of the adenylate binding sites is expected with a concomitant decreased capability to bind 2-OG. In agreement, the number of 2-OG binding sites per P_{II} trimer was reduced by the addition of ADP. As long as ATP stayed in excess over ADP, the 2-OG binding process could be fitted according to a three sequential binding model, but the average number of 2-OG-binding sites in the mixed population of P_{II} trimers decreased. This indicates that part of the P_{II} population didn't exhibit three 2-OG binding sites anymore. This part of the population has probably at least one ADP molecule bound. Furthermore, the affinity for 2-OG binding decreases. At a 1:1 molar ratio of ADP to ATP, the dominating P_{II} population should consist of P_{II} trimers with a mixed occupation of ATP and ADP. Considering the 2-3-higher affinity for ATP, the P_{II} species P_{II}-ATP_2ADP_1 should clearly prevail over the species P_{II}-ATP_1ADP_2. Under these conditions, on average, only one 2-OG molecule can apparently bind to P_{II}. The binding process can no more be fitted according to a three sequential binding site model. The affinity of the remaining 2-OG-binding site seems to be as low as that of the third, low-affinity 2-OG-binding site of ATP-ligated P_{II} (Tab. 1). This implies that binding of ADP to one site in P_{II} has a strong negative effect for the remaining 2-OG-binding sites, so that probably only one site can be efficiently occupied. The binding of 2-OG to the lowest affinity site appears to be crucial for inhibition of P_{II}-NAGK interaction, since the IC_{50} of 2-OG at a 1:1 ratio of ADP to ATP (145 µM) for inhibiting P_{II}-NAGK interaction is near the K_d measured for 2-OG binding at the same ADP/ATP concentrations (183 µM). This mechanism allows the P_{II}-NAGK complex to stay sensitive towards 2-OG under low energy conditions.

The ADP-ligated P_{II} protein appears to be able to bind to NAGK, but binding is clearly different for that of ATP-ligated P_{II}, as revealed by SPR spectroscopy. In particular, the dissociation rate of the P_{II}-NAGK complex was highly increased by ADP. The increased dissociation rate results in a lower steady state binding level of P_{II}-ADP to NAGK. P_{II}-species occupied with a mixture of ATP and ADP display intermediate binding properties: At 1:2 and 2:2 mM mixtures of ADP/ATP, the P_{II}-ATP_2ADP_1 species should prevail. These conditions already lead to enhanced complex dissociation. In mixtures of 3:2 or 4:2 mM ADP/ATP, more and more of the P_{II}-ATP_1ADP_2 species should appear, however, fully ADP-ligated P_{II} species are very unlikely. In accord, the binding curves under these two conditions were very similar towards each other and distinct from that of fully ADP-ligated P_{II} with NAGK.

We have previously suggested a two-step model for the binding of P_{II} to NAGK [6]. Following a transient encounter complex involving B-loop residues of P_{II}, the T-loop folds into a compact conformation, which tightly associates with NAGK. In ADP-ligated P_{II} protein, the T-loop may be impaired in folding into the perfect NAGK-binding conformation, explaining the fast dissociation of the complex. Measuring NAGK activity in mixtures of ATP, ADP and P_{II} suggests that P_{II} protein occupied with ATP/ADP mixtures is unable to enhance the catalytic activity of NAGK. On the other hand, NAGK, which forms a complex with ATP/ADP-occupied P_{II} is protected from arginine inhibition as efficient as by purely ATP-occupied P_{II}. These properties suggest that protection from arginine inhibition and activation of catalytic activity of NAGK by P_{II} operates by

different mechanisms: The loose binding of ATP/ADP-ligated P_{II} to NAGK is sufficient to relieve arginine inhibition, but is insufficient to rearrange the catalytic centre of NAGK, resulting in enhanced activity. This suggestion is in accord with two different contact surfaces of P_{II} with NAGK [35]. The rearrangement of the catalytic centre of NAGK by P_{II} has been shown to require a tight hydrogen-bonding and ion-pair network involving the distal part of the T-loop of P_{II} and the N-domain of NAGK, tightening the catalytic centre of NAGK [35]. The inability of ATP/ADP-ligated P_{II} to enhance NAGK activity is thus in accord with the lax binding of this P_{II} species, probably mediated by imperfect fit of the T-loop to the corresponding NAGK recognition site. By contrast, the relief from arginine inhibition appears to be mediated by the C-terminus of NAGK [36], interacting with the body of the P_{II} protein. In essence, NAGK complexed to partially ADP-ligated P_{II} is not catalytically induced but still relived from feedback inhibition by arginine. In such a state, P_{II}-complexed NAGK wouldn't support elevated arginine synthesis for efficient nitrogen storage but could quickly respond to increasing energy levels.

PipX is another known partner of P_{II} protein in *S. elongatus*. It switches between binding to P_{II} or NtcA, depending on the 2-OG concentration. Low adenylate energy charge (increased ADP/ATP ratio) enhances the association of the P_{II}-PipX complex *in vitro,* thereby antagonizing the signal of nitrogen limitation (elevated 2-OG levels). P_{II}-PipX complex formation is highly ADP-sensitive; ADP promotes complex formation and protects it from dissociation by 2-OG *in vitro*. Therefore, increasing ADP levels should decrease the activation of NtcA-dependent genes, which depends of PipX-NtcA interaction, due to efficient competition of P_{II} for PipX. Remarkably, the negative effect of 2-OG on P_{II}-PipX interaction was absent when Strep-tagged P_{II} was fixed with its C-terminus to the sensor surface but could partially be restored with heterotrimeric Strep-tagged P_{II}, which consists partially of untagged monomers with a free C-terminus. Although P_{II}-PipX binding itself doesn't involve conformational changes on the C-terminus of P_{II}, the movement of the C-terminus imposed by 2-OG binding is essential for the response to the effector molecules and incorporating metabolic signals [8, 9]. Together, this study shows how the *S. elongatus* P_{II} signal transduction protein is capable to respond in a fine-tuned manner to the change of the energy charge *in vitro*. Through P_{II}-dependent adenylate energy signalling, increasing ADP levels should diminish the NtcA-dependent activation of genes required for nitrogen assimilation under nitrogen-limiting conditions (high 2-OG levels). On the other hand, under nitrogen-excess conditions (low 2-OG levels), increased ADP levels, via P_{II} signalling, should diminish the activation of NAGK, thereby reducing the flux into the arginine biosynthesis pathway. In both cases, P_{II}-dependent signalling of increased ADP levels should dampen energetically expensive anabolic reactions. Comparing the response of PipX and NAGK to EC signalling by P_{II}, it appears that PipX is more sensitive towards low ADP levels.

The ability to bind 2-OG and adenyl nucleotides is conserved among P_{II} proteins in all three domains of life. Several studies indicated the involvement of P_{II} in sensing the energy status in various bacteria. It was suggested that P_{II} proteins in photosynthetic Proteobacterium *Rhodospirillum rubrum* responds to the cellular energy charge [22, 45]. Mutants of *Rhodospirillum rubrum* with impaired purine synthesis pathway were created and than provided with an exogenous adenine source to test the effect of different cellular ATP levels on P_{II} signal transduction. However, depleted ATP levels had little effect on P_{II}-mediated regulation of NifA and nitrogenase activity. It was suggested that the ADP/ATP ratio states the actual signal for P_{II} protein, but the direct effect of ADP/ATP ratios has not been shown yet [5]. Jiang and Ninfa showed for the first time with reconstituted signal transduction systems using the *E. coli* P_{II} protein and its receptors NtrB, ATase and UTase/UR, that ADP affected almost all signalling properties of *E. coli* P_{II} by antagonizing 2-OG mediated responses [3, 18]. The metabolite sensing involves intersubunit signalling in the P_{II} trimer itself with cooperation of the multiple effector binding sites [19]. Furthermore, ADP antagonized the inhibitory effect of 2-oxoglutarate on the binding of the P_{II} paralogue GlnK to the AmtB ammonium transport protein in E. coli [7]. The present study extends these insights: in the

case of the cyanobacterial system, ADP does not always antagonize the 2-OG signal but differentially affects the interaction of P_{II} with its targets. ADP modulates P_{II} signalling to the receptor NAGK primarily at low 2-OG levels without antagonizing the effect of 2-OG, whereas it antagonizes the inhibitory effect of 2-OG for P_{II}-PipX interaction. There is still discussion on how much unbound ATP is available in the cell at any given moment [46], but it appears that the ratio of ADP to ATP instead of the absolute concentration of ATP affects P_{II} signal transduction. Further studies using *in vivo* systems could shed light on the physiological impact of this remarkable and complex signalling system.

Acknowledgements

We thank Christopher Schuster and Sebastian Kindermann for their help in creating the heterotrimeric Strep-tagged P_{II} protein.

Funding

This work was supported by DFG grant Fo195/10.

Numbered references

1 Chapman, A. G., Fall, L. and Atkinson, D. E. (1971) Adenylate energy charge in *Escherichia coli* during growth and starvation. J. Bacteriol. **108**, 1072-1086

2 Franzen, J. S. and Binkley, S. B. (1961) Comparison of the acid-soluble nucleotides in *Escherichia coli* at different growth rates. J. Biol. Chem. **236**, 515-519

3 Jiang, P. and Ninfa, A. J. (2007) *Escherichia coli* P_{II} signal transduction protein controlling nitrogen assimilation acts as a sensor of adenylate energy charge *in vitro*. Biochemistry. **46**, 12979-12996

4 Forchhammer, K. (2008) P(II) signal transducers: novel functional and structural insights. Trends Microbiol. **16**, 65-72

5 Zhang, Y., Pohlmann, E. L. and Roberts, G. P. (2009) Effect of perturbation of ATP level on the activity and regulation of nitrogenase in *Rhodospirillum rubrum*. J. Bacteriol. **191**, 5526-5537

6 Fokina, O., Chellamuthu, V. R., Zeth, K. and Forchhammer, K. (2010) A Novel Signal Transduction Protein P(II) Variant from *Synechococcus elongatus* PCC 7942 Indicates a Two-Step Process for NAGK-P(II) Complex Formation. J. Mol. Biol. **399**, 410-421

7 Radchenko, M. V., Thornton, J. and Merrick, M. (2010) Control of AmtB-GlnK complex formation by intracellular levels of ATP, ADP, and 2-oxoglutarate. J. Biol. Chem. **285**, 31037-31045

8 Fokina, O., Chellamuthu, V. R., Forchhammer, K. and Zeth, K. (2010) Mechanism of 2-oxoglutarate signaling by the *Synechococcus elongatus* P_{II} signal transduction protein. Proc. Natl. Acad. Sci. U. S. A. **107**, 19760-19765

9 Truan, D., Huergo, L. F., Chubatsu, L. S., Merrick, M., Li, X. D. and Winkler, F. K. (2010) A new P(II) protein structure identifies the 2-oxoglutarate binding site. J. Mol. Biol. **400**, 531-539

10 Ninfa, A. J. and Jiang, P. (2005) P_{II} signal transduction proteins: sensors of alpha-ketoglutarate that regulate nitrogen metabolism. Curr. Opin. Microbiol. **8**, 168-173

11 Leigh, J. A. and Dodsworth, J. A. (2007) Nitrogen regulation in bacteria and archaea. Annu. Rev. Microbiol. **61**, 349-377

12 Sant'Anna, F. H., Trentini, D. B., de Souto Weber, S., Cecagno, R., da Silva, S. C. and Schrank, I. S. (2009) The P_{II} superfamily revised: a novel group and evolutionary insights. J. Mol. Evol. **68**, 322-336

13 Forchhammer, K. (2004) Global carbon/nitrogen control by P_{II} signal transduction in cyanobacteria: from signals to targets. FEMS Microbiol. Rev. **28**, 319-333

14 Xu, Y., Cheah, E., Carr, P. D., van Heeswijk, W. C., Westerhoff, H. V., Vasudevan, S. G. and Ollis, D. L. (1998) GlnK, a P_{II}-homologue: structure reveals ATP binding site and indicates how the T-loops may be involved in molecular recognition. J. Mol. Biol. **282**, 149-165

15 Xu, Y., Carr, P. D., Clancy, P., Garcia-Dominguez, M., Forchhammer, K., Florencio, F., Vasudevan, S. G., Tandeau de Marsac, N. and Ollis, D. L. (2003) The structures of the P_{II} proteins from the cyanobacteria *Synechococcus* sp. PCC 7942 and *Synechocystis* sp. PCC 6803. Acta. Crystallogr. D. Biol. Crystallogr. **59**, 2183-2190

16 Sakai, H., Wang, H., Takemoto-Hori, C., Kaminishi, T., Yamaguchi, H., Kamewari, Y., Terada, T., Kuramitsu, S., Shirouzu, M. and Yokoyama, S. (2005) Crystal structures of the signal transducing protein GlnK from *Thermus thermophilus* HB8. J. Struct. Biol. **149**, 99-110

17 Forchhammer, K. and Hedler, A. (1997) Phosphoprotein P_{II} from cyanobacteria--analysis of functional conservation with the P_{II} signal-transduction protein from *Escherichia coli*. Eur. J. Biochem. **244**, 869-875

18 Jiang, P. and Ninfa, A. J. (2009) Alpha-Ketoglutarate Controls the Ability of the *Escherichia coli* P_{II} Signal Transduction Protein To Regulate the Activities of NRII (NtrB) but Does Not Control the Binding of P_{II} to NRII. Biochemistry. **48**, 11514-11521

19 Jiang, P. and Ninfa, A. J. (2009) Sensation and Signaling of alpha-Ketoglutarate and Adenylylate Energy Charge by the *Escherichia coli* P_{II} Signal Transduction Protein Require Cooperation of the Three Ligand-Binding Sites within the P_{II} Trimer. Biochemistry. **48**, 11522-11531

20 Smith, C. S., Weljie, A. M. and Moorhead, G. B. (2003) Molecular properties of the putative nitrogen sensor P_{II} from *Arabidopsis thaliana*. Plant J. **33**, 353-360

21 Zhang, Y., Pohlmann, E. L., Halbleib, C. M., Ludden, P. W. and Roberts, G. P. (2001) Effect of P(II) and its homolog GlnK on reversible ADP-ribosylation of dinitrogenase reductase by heterologous expression of the *Rhodospirillum rubrum* dinitrogenase reductase ADP-ribosyl transferase-dinitrogenase reductase-activating glycohydrolase regulatory system in Klebsiella pneumoniae. J. Bacteriol. **183**, 1610-1620

22 Zhang, Y., Pohlmann, E. L., Ludden, P. W. and Roberts, G. P. (2001) Functional characterization of three GlnB homologs in the photosynthetic bacterium *Rhodospirillum rubrum*: roles in sensing ammonium and energy status. J. Bacteriol. **183**, 6159-6168
23 Zhang, Y. P., Pohlmann, E. L., Ludden, P. W. and Roberts, G. P. (2003) Regulation of nitrogen fixation by multiple P-II homologs in the photosynthetic bacterium *Rhodospirillum rubrum*. Symbiosis. **35**, 85-100
24 Kloft, N. and Forchhammer, K. (2005) Signal transduction protein P-II phosphatase PphA is required for light-dependent control of nitrate utilization in *Synechocystis* sp strain PCC 6803. Journal of Bacteriology. **187**, 6683-6690
25 Takatani, N., Kobayashi, M., Maeda, S. I. and Omata, T. (2006) Regulation of nitrate reductase by non-modifiable derivatives of P_{II} in the cells of *Synechococcus elongatus* strain PCC 7942. Plant and Cell Physiology. **47**, 1182-1186
26 Espinosa, J., Forchhammer, K., Burillo, S. and Contreras, A. (2006) Interaction network in cyanobacterial nitrogen regulation: PipX, a protein that interacts in a 2-oxoglutarate dependent manner with P_{II} and NtcA. Mol. Microbiol. **61**, 457-469
27 Espinosa, J., Forchhammer, K. and Contreras, A. (2007) Role of the *Synechococcus* PCC 7942 nitrogen regulator protein PipX in NtcA-controlled processes. Microbiology-Sgm. **153**, 711-718
28 Llacer, J. L., Espinosa, J., Castells, M. A., Contreras, A., Forchhammer, K. and Rubio, V. (2010) Structural basis for the regulation of NtcA-dependent transcription by proteins PipX and P_{II}. Proc. Natl. Acad. Sci. U. S. A. **107**, 15397-15402
29 Burillo, S., Luque, I., Fuentes, I. and Contreras, A. (2004) Interactions between the nitrogen signal transduction protein P_{II} and N-acetyl glutamate kinase in organisms that perform oxygenic photosynthesis. J. Bacteriol. **186**, 3346-3354
30 Heinrich, A., Maheswaran, M., Ruppert, U. and Forchhammer, K. (2004) The *Synechococcus elongatus* P signal transduction protein controls arginine synthesis by complex formation with N-acetyl-L-glutamate kinase. Mol. Microbiol. **52**, 1303-1314
31 Maheswaran, M., Urbanke, C. and Forchhammer, K. (2004) Complex formation and catalytic activation by the P_{II} signaling protein of N-acetyl-L-glutamate kinase from *Synechococcus elongatus* strain PCC 7942. J. Biol. Chem. **279**, 55202-55210
32 Chen, Y. M., Ferrar, T. S., Lohmeier-Vogel, E. M., Morrice, N., Mizuno, Y., Berenger, B., Ng, K. K. S., Muench, D. G. and Moorhead, G. B. G. (2006) The P_{II} signal transduction protein of *Arabidopsis thaliana* forms an arginine-regulated complex with plastid N-acetyl glutamate kinase.(vol 281, pg 5726, 2006). Journal of Biological Chemistry. **281**, 24084-24084
33 Bourrellier, A. B. F., Valot, B., Guillot, A., Ambard-Bretteville, F., Vidal, J. and Hodges, M. (2010) Chloroplast acetyl-CoA carboxylase activity is 2-oxoglutarate-regulated by interaction of P_{II} with the biotin carboxyl carrier subunit. Proc. Natl. Acad. Sci. U. S. A. **107**, 502-507
34 Mizuno, Y., Moorhead, G. B. and Ng, K. K. (2007) Structural basis for the regulation of N-acetylglutamate kinase by P_{II} in *Arabidopsis thaliana*. J. Biol. Chem. **282**, 35733-35740
35 Llacer, J. L., Contreras, A., Forchhammer, K., Marco-Marin, C., Gil-Ortiz, F., Maldonado, R., Fita, I. and Rubio, V. (2007) The crystal structure of the complex of P_{II} and acetylglutamate kinase reveals how P_{II} controls the storage of nitrogen as arginine. Proc. Natl. Acad. Sci. U. S. A. **104**, 17644-17649
36 Beez, S., Fokina, O., Herrmann, C. and Forchhammer, K. (2009) N-acetyl-L-glutamate kinase (NAGK) from oxygenic phototrophs: P(II) signal transduction across domains of life reveals novel insights in NAGK control. J. Mol. Biol. **389**, 748-758
37 Forchhammer, K. and Demarsac, N. T. (1995) Functional-Analysis of the Phosphoprotein P-Ii (Glnb Gene-Product) in the Cyanobacterium *Synechococcus* Sp Strain Pcc-7942. Journal of Bacteriology. **177**, 2033-2040
38 Forchhammer, K. and Demarsac, N. T. (1995) Phosphorylation of the P-Ii Protein (Glnb Gene-Product) in the Cyanobacterium *Synechococcus* Sp Strain Pcc-7942 - Analysis of *in vitro* Kinase-Activity. Journal of Bacteriology. **177**, 5812-5817
39 Ruppert, U., Irmler, A., Kloft, N. and Forchhammer, K. (2002) The novel protein phosphatase PphA from *Synechocystis* PCC 6803 controls dephosphorylation of the signalling protein P-II. Molecular Microbiology. **44**, 855-864
40 Forchhammer, K., Irmler, A., Kloft, N. and Ruppert, U. (2004) P-II signalling in unicellular cyanobacteria: analysis of redox-signals and energy charge. Physiologia Plantarum. **120**, 51-56
41 Bueno, R., Pahel, G. and Magasanik, B. (1985) Role of *glnB* and *glnD* gene products in regulation of the glnALG operon of *Escherichia coli*. J. Bacteriol. **164**, 816-822
42 Studier, F. W., Rosenberg, A. H., Dunn, J. J. and Dubendorff, J. W. (1990) Use of T7 RNA polymerase to direct expression of cloned genes. Methods Enzymol. **185**, 60-89
43 Takahara, K., Akashi, K. and Yokota, A. (2007) Continuous spectrophotometric assays for three regulatory enzymes of the arginine biosynthetic pathway. Analytical Biochemistry. **368**, 138-147
44 Forchhammer, K. and Demarsac, N. T. (1994) The P-Ii Protein in the Cyanobacterium *Synechococcus* Sp Strain Pcc-7942 Is Modified by Serine Phosphorylation and Signals the Cellular N-Status. Journal of Bacteriology. **176**, 84-91

45 Zhang, Y., Wolfe, D. M., Pohlmann, E. L., Conrad, M. C. and Roberts, G. P. (2006) Effect of AmtB homologues on the post-translational regulation of nitrogenase activity in response to ammonium and energy signals in *Rhodospirillum rubrum*. Microbiology. **152**, 2075-2089

46 Schneider, D. A. and Gourse, R. L. (2004) Relationship between growth rate and ATP concentration in *Escherichia coli* - A bioassay for available cellular ATP. Journal of Biological Chemistry. **279**, 8262-8268

Figure legends

Figure 1 Effect of ADP on NAGK activity in the AGPR-coupled assay
Assay was performed in the presence of ATP at a concentration of 4 mM (dashed line), 2 mM (solid line), 1 mM (dotted line) and 0.5 mM (dot-dashed line), as indicated. AGPR-coupled NAGK assays were performed as described in Experimental. The percents of NAGK activity were plotted against the respective analyte concentration (standard deviations from the different measurements for each data point are indicated by error bars) and the data points were fitted to a hyperbolic curve (**a**) Enzyme activity with P_{II} protein (**b**) Effect on NAGK without P_{II}.

Figure 2 Arginine inhibition and antagonistic effect of 2-OG on the NAGK activation by P_{II} in the presence of arginine
AGPR-coupled NAGK assays were performed as described in Experimental. The percents of the NAGK activity were plotted against the respective analyte concentration (standard deviations from the different measurements for each data point are indicated by error bars) and the data points were fitted to a hyperbolic curve (**a**) ADP enhances inhibition of the NAGK activity by arginine in the presence of 2 mM ATP. NAGK activity in the absence of P_{II} and ADP (solid line), in the presence of P_{II}: without ADP (dashed line), with 0.5 mM ADP (dotted line), with 1 mM ADP (thin solid line), with 2 mM ADP (dot-dashed line), with 4 mM ADP (dot-dot-dashed line). NAGK activity in the absence P_{II} and arginine (dot-dashed line) (**b**) 2-OG effect on NAGK induction by P_{II} in the presence of 2 mM ATP and 30 µM arginine without ADP (solid line) and with 2 mM ADP (dashed line).

Figure 3 ITC measurement of the 2-OG binding to P_{II} protein
The upper panels show the raw data in the form of the heat effect during the titration of 33 µM P_{II} solution (trimer concentration) with 2 mM 2-OG. The lower panels show the binding isotherm and the best-fit curve according to the one-site binding model (**a**) 2-OG binding (titration 4.2-293.7 µM) in the presence of 1 mM ATP (**b**) 2-OG binding in the presence of 1 mM ADP (**c**), (**d**) and (**e**) 2-OG binding in the presence of 1 mM ATP and 0.25 mM (C), 0.5 mM (D), 1 mM (E) ADP.

Figure 4 SPR analysis of the ADP/ATP ratio influence on the association and the dissociation of the P_{II}-NAGK complex
NAGK was bound to FC2 of a Ni^{2+} -loaded NTA sensor chip (see Experimental) and FC1 was used as a background control. The response difference (ΔRU) between FC1 and FC2 is shown (**a**) Effect of 1 mM ADP on the dissociation of wt P_{II}-NAGK complex following association without effectors (left) and in the presence of 1 mM ADP (right) (**b**) Association and dissociation of P_{II}-NAGK complex under influence of different ADP/ATP ratios: 2 mM ATP (solid line), 2 mM ATP + 1 mM ADP (dotted line), 2 mM ATP + 2 mM ADP (short dashed line), 2 mM ATP + 4 mM ADP (long dashed line) and 2 mM ADP (dot-dashed line).

Figure 5 Effect of ATP, ADP and 2-OG on P_{II}-PipX complex formation
(**a**) His_6-PipX (500 nM) was preincubated with homotrimeric Strep-P_{II} (100 nM) in the absence or in the presence of effectors, as indicated, and injected on the Ni^{2+}-loaded NTA chip for SPR detection. As a control, His_6-PipX was injected under the same conditions, but in the absence of P_{II}. The response signal at t = 197 s after start of the injection phase was taken as a measure of protein binding. The binding of His_6-PipX alone was subtracted from the results measured in the presence of P_{II}. Error bars indicate standard deviations from the three independent measurements. (**b**) P_{II}-PipX binding assay using the glutardialdehyde cross-linking *in vitro*. P_{II} was preincubated with PipX in the presence and in the absence of effectors, as indicated, and subsiqently cross-linked using glutardialdehyde. The cross-link products were analyzed by SDS-PAGE followed by immunoblot analysis with P_{II}-specific antibody. (**c**) Effect of ADP, ATP and 2-OG on PipX binding to immobilized heterotrimeric Strep-tagged P_{II} protein. P_{II} (3.2 µM) was bound to FC2 of a CM5

chip and FC1 was used as a background control. The response difference (ΔRU) between FC1 and FC2 is shown. PipX (2 μM) was injected in absence of effector molecules (solid line), in the presence of 2 mM ADP (long dashed line), 2 mM ATP + 1 mM 2-OG (middle dashed line), 2 mM ADP + 2 mM ATP + 1 mM 2-OG (short dashed line) and 4 mM ADP + 2 mM ATP + 1 mM 2-OG (dotted line)

Figure S1 SPR detection of P_{II}-PipX complexes using Ni^{2+}-loaded NTA chip
His_6-PipX (500 nM) was preincubated with homotrimeric Strep-P_{II} (100 nM) in the absence (dotted line) and in the presence of 1 mM ADP (dashed line) and injected on the Ni^{2+}-loaded NTA chip. Solid line corresponds to the control binding experiment of His_6-PipX in the absence of P_{II}. The sensorgram shows the increase of RU (resonance units) that represents the protein binding to the chip surface. The difference in the RU between binding experiments in the presence of P_{II} and the control (PipX alone) at t=197 s, indicated by an arrow, was used to quantify the amount of PipX-P_{II} complex formation.

Figure S2 SPR detection of P_{II}-PipX complexes using CM5 chip
Homotrimeric Step-P_{II} (3.2 μM) was immobilized to FC2 of the Strep-Tactin-coated CM5 chip and FC1 was used as a background control. His_6-PipX (2 μM) was injected in absence of effector molecules (solid line), in the presence of 1 mM ATP (dotted line) and of 1 mM ATP + 1 mM 2-OG (dashed line).

Biochemical Journal Immediate Publication. Published on 21 Jul 2011 as manuscript BJ20110536

Tables and Figures

Table 1 2-OG binding to P_{II} in the presence of various ADP/ATP ratios

Values correspond to the mean of three experiments ± SEM. The raw data were fitted using one-site and three-sites binding models for a P_{II} trimer. For comparison, the 2-OG binding in the presence of 1 mM ATP data fitted according to the three sites binding model are given in parentheses. NF, non fittable.

	one-site binding model		three-sites binding model		
ADP:ATP	N, sites	K_d, µM	K_d1, µM	K_d2, µM	K_d3, µM
0:1	1.725 ± 0.01	38.9 ± 1.1	(5.1 ± 4.0)	(11.1 ± 1.8)	(106.7 ± 14.8)
0.25:1	1.35 ± 0.16	78.2 ± 18	12.2 ± 6.4	41.2 ± 28.8	263.5 ± 153.1
0.5:1	1.125 ± 0.15	95.0 ± 16.5	11.0 ± 6.0	19.8 ± 2.1	194.9 ± 45.0
1:1	0.75 ± 0.26	182.9 ± 4.3		NF	

Figure 1

A

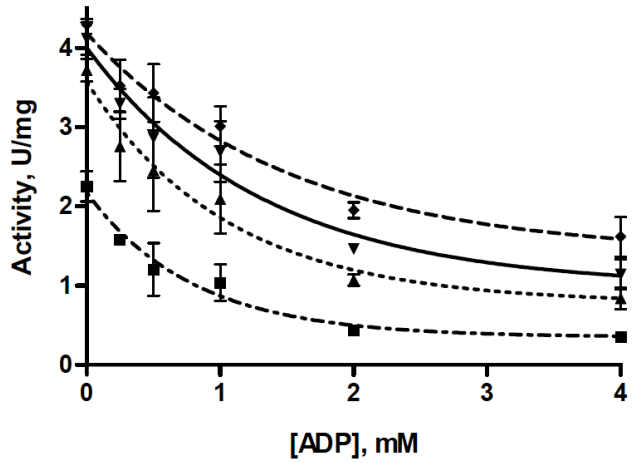

B

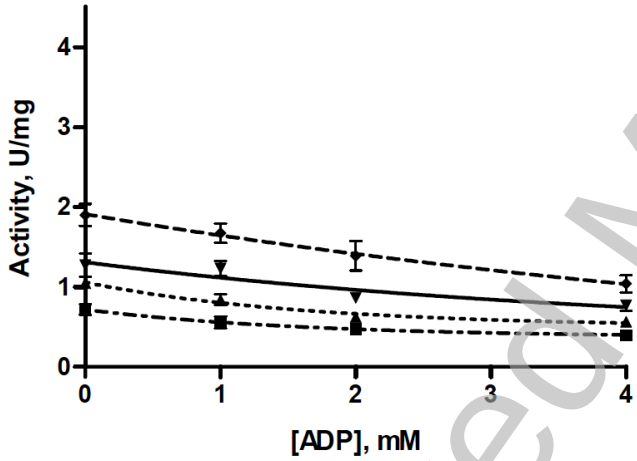

Figure 2

A

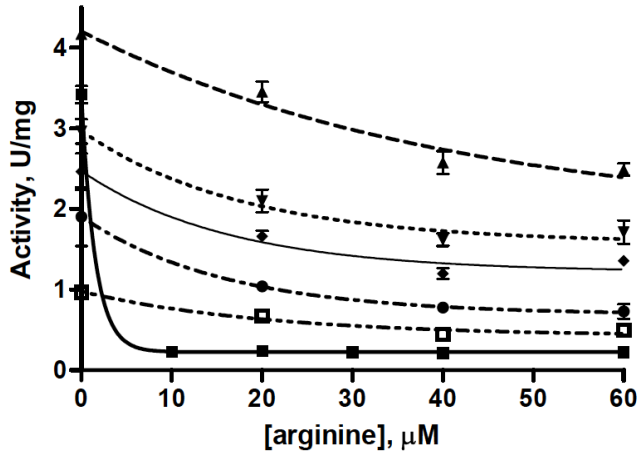

B

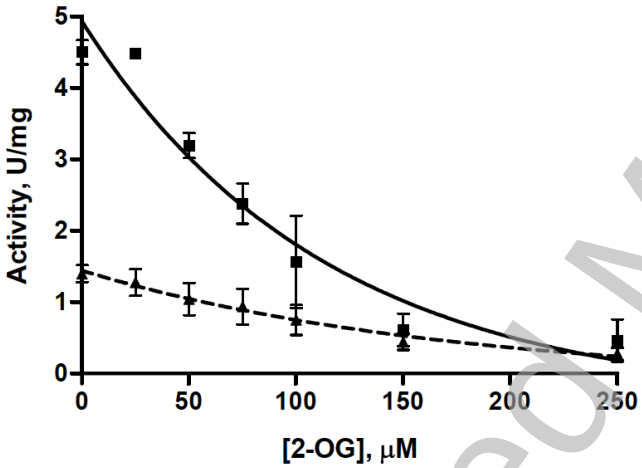

Figure 3

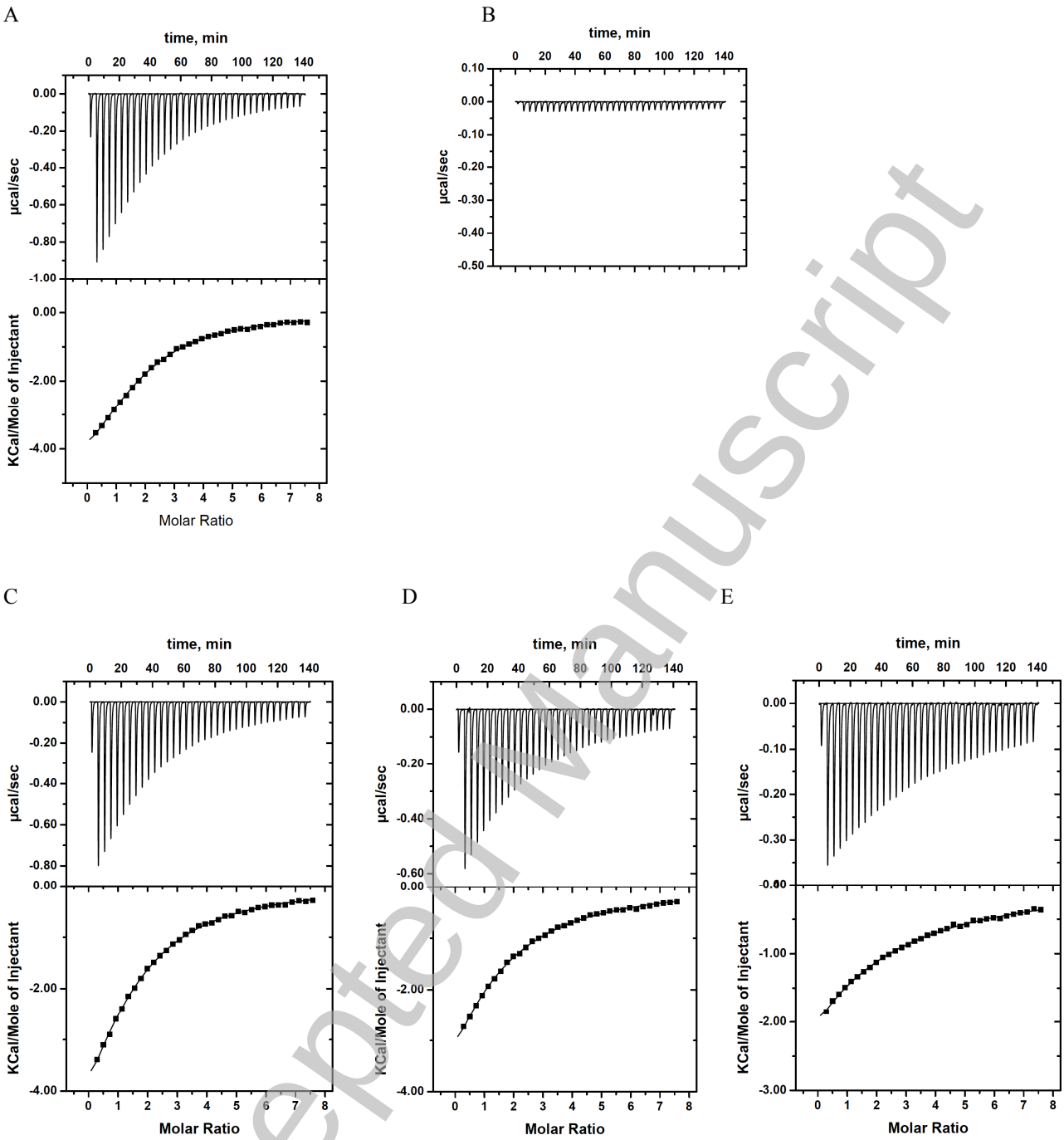

Figure 4

A

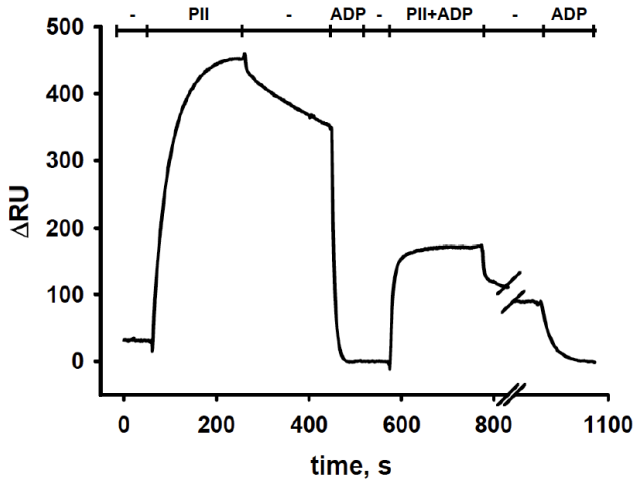

B

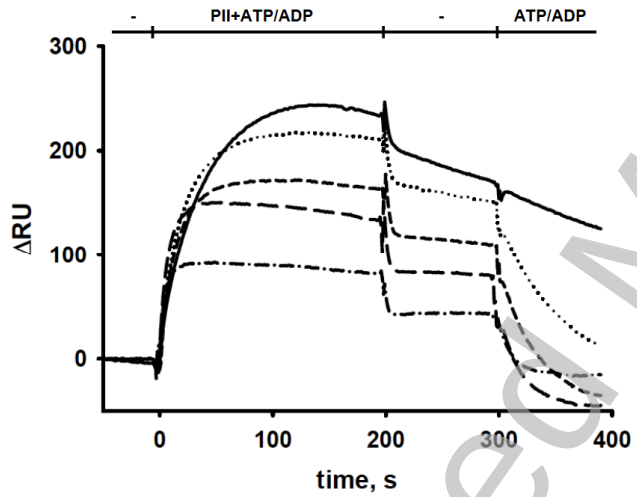

Figure 5

A

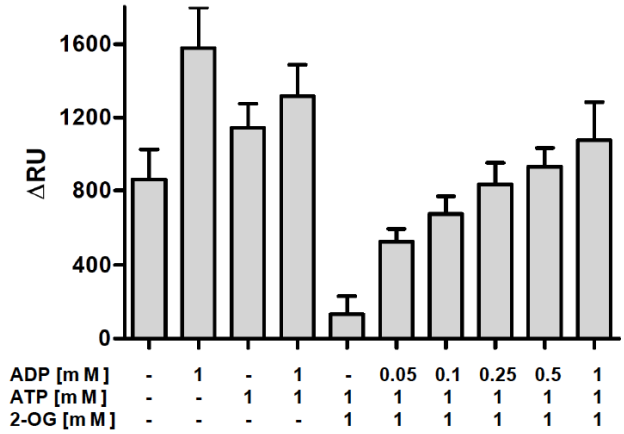

B

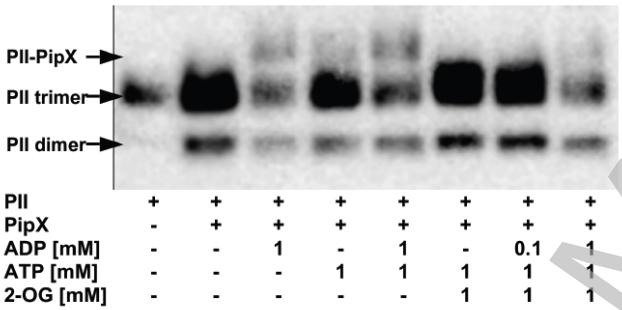

C